Liu, Y., Cao, Q., Liu, W., Lin, C.-H., Wei, D., Baughcum, S., Norris, S., Long, Z., Shen, X., and Chen, Q. 2017. "Numerical modeling of particle deposition in the environmental control systems of commercial airliners on ground," *Building Simulation,* 10(2): 265-275..

Numerical Modeling of Particle Deposition in the Environmental Control Systems of Commercial Airliners on Ground

Yudi Liu[a], Qing Cao[a], Wei Liu[a,b], Chao-Hsin Lin[c], Daniel Wei[d], Steven Baughcum[c], Sharon Norris[c], Zhengwei Long[a], Xiong Shen[a,*], and Qingyan Chen[a,b]
[a] *Tianjin Key Laboratory of Indoor Air Environmental Quality Control, School of Environmental Science and Engineering, Tianjin University, Tianjin, China*
[b] *School of Mechanical Engineering, Purdue University, West Lafayette, IN, USA*
[c] *The Boeing Company, Seattle, USA*
[d] *Boeing Research & Technology-China, Beijing, China*
**Corresponding email: shenxiong@tju.edu.cn*

HIGHLIGHTS

- A generic numerical model based on empirical equations was developed for calculating particle deposition in aircraft environmental control system with common components.
- Particle deposition in ECSs was studied for five types of commercial airplanes.
- The numerical results were compared with experimental data for particle deposition.

Abstract

The environmental control system (ECS) of a commercial airplane supplies air to the cabin in order to maintain a safe, comfortable, and healthy environment for passengers and crew members. Because about half of the air supplied to the cabin is outside air, atmosphere particles could deposit in the ECS before entering the cabin. This investigation developed a model to calculate the particle deposition rates in the ECS for different particle sizes on the basis of a set of empirical equations from the literature. The model was used to predict particle deposition in five types of commercial airplanes (a regional jet, Boeing 737-800, Airbus 319, Airbus 320, and MD-82). The predicted results were compared with data measured in-flight or during operation on the ground and agreed well with the measured data. Both the simulated and measured results showed that almost all the large particles ($d_p \geq 5.0$ μm) and 75% of small particles（d_p=0.3-5.0 μm）were deposited in the ECS. Most of the particle deposition occurred near the entrance to the ECS where the geometry was the most complex.

Keywords: Airplane, Environmental control system, Air quality, Particulate matter, Deposition

Nomenclature			
A	Inner surface area of the duct section(m^2)	St	Stokes number
a, b, c, d	Coefficient related to curvature ratio	Stk_{fin}	Stokes number based on the duct air velocity and the fin thickness
C	Particle mass/number concentration	t_{fin}	Fin thickness (m)
C_c	Cunningham factor	u_m	Average flow velocity in the duct (m/s)
cf	Corrugation factor	u^*	Friction velocity (m/s)
D	Diameter of the duct (m)	V	Volume of the duct section (m^3)
d_p	Particle aerodynamic diameter (μm)	v_d	Particle deposition velocity (m/s)
d_0	Hydraulic diameter of the duct (m)	v_d^+	Dimensionless particle deposition velocity
d^+	Dimensionless particle diameter		
f	Friction factor	w	Center-to-center fin spacing (m)
f'	Intermediate variable	***Greek symbols***	
g^+	Dimensionless gravitational force	δ	Curvature ratio
k	Absolute roughness (m)	η	Particle deposition rate (1/s)
k^+	Dimensionless roughness	η_d	Particle deposition percent rate
L	Length of the duct (m)	θ	Surface inclination angle (°)
L_1^+	Dimensionless lift force	θ'	Angle of the curved pipe (°)
P	Particle penetration rate	λ	Mean free path of air molecule (m)
R	Curve radius	μ	Dynamic viscosity (Pa·s)
Re	Reynolds number	ν	Kinematic viscosity (m^2/s)
S	Particle-to-gas density ratio	ρ_p	Particle density (kg/m^3)
Sc	Schmidt number	τ_p^+	Dimensionless particle relaxation time

1 Introduction

China is facing a very serious air pollution problem, with enormous amounts of suspended particulate matter (PM) in the air (Kan, H., Chen, B., & Hong, C., 2009). The PM includes airborne dust, soot, and other pollutants that have condensed in the atmosphere. $PM_{2.5}$ is defined as the total mass of particles that are less than 2.5 microns in diameter, while PM_{10} is the total mass of particles that are less than 10 microns in diameter. The China National Environmental Monitoring Center (CNEMC, 2014) found that the average concentration of particulate matter with a diameter smaller than 2.5 μm ($PM_{2.5}$) in 74 major Chinese cities was 76 $\mu g/m^3$ in the first half of 2013, which was about three times higher than the standard ($\leq$ 25 $\mu g/m^3$) set by the World Health Organization.

We calculated the $PM_{2.5}$ and PM_{10} mass concentration data at six major airports in China (Beijing, Shanghai Pudong, Shanghai Hongqiao, Shenzhen, Guangzhou, and Tianjin) for a period of a year starting on October 18, 2013 using data from the three nearest monitoring sites of the China National Environmental Monitoring Center for each airport to understand the air quality at airports in China. The data shows that the average $PM_{2.5}$ and PM_{10} mass concentrations were 63.1 $\mu g/m^3$ and 93.3 $\mu g/m^3$, respectively, while the standards set by the World Health Organization were 25 $\mu g/m^3$ for $PM_{2.5}$ and 50 $\mu g/m^3$ for PM_{10}. This heavy air pollution has a major impact on environmental control system (ECS) of commercial airplanes as the flight delays in China's airspace were very severe. According to data from FlightStats (2014), an average of 39 % flights were delayed in China, with an average delay time of 56 minutes.

When an aircraft is delayed on the ground before taking off, more particles from the outside air enter the ECS through the jet-bridge air-conditioning packages (JAPs), ground air-conditioning carts (GACs), engines, or auxiliary power units (APUs) which include similar components with engines. Since the JAPs, GACs, and APUs do

not have high-efficiency particulate air (HEPA) filters for fine particles, such particles could deposit in the ECS, and some could enter the cabin. Furthermore, whereas a JAP or GAC can be easily maintained, servicing an APU and ECS can be difficult because it is a system of the airplane. Therefore, it is important to study where the particles were deposited in APU and ECS so that proper measures can be developed to ensure their safe operation and efficiency. The study of particle penetration to aircraft cabin will help us to determine if a risk assessment on the exposure of passengers and crew is needed.

Multiple studies have been conducted on particle deposition and penetration in ECSs in buildings and airplanes. There are primarily three types of models for simulating particle deposition, namely, analytical models, computational fluid dynamics (CFD) models, and empirical equations. Lai (2003) reviewed a number of studies of indoor particle deposition in non-industrial environments. The models obtained in these studies were mainly analytical equations with a complex form which usually applied to simple geometries. Zhao and Chen (2006) used a three-dimensional drift-flux model in CFD to analyze particle deposition in a ventilation duct, and they obtained good results as compared with experimental data. Several other investigations studied particle deposition by using CFD with different particle models (Tian & Ahmadi, 2007; Zhang, J., Li, A., & Li, D., 2008; Sun, K., Lu, L., & Jiang, H., 2011; Wang, M., Lin, C.-H., & Chen, Q, 2011). Although the simulated results in these studies were good, building geometric models for CFD could be very difficult because of the detailed information that is needed. Another disadvantage is the intensive computing effort required by CFD simulations. On the other hand, empirical equations are based on sound physical principles, and they can account for the impact of most of the important parameters of particle deposition, such as surface roughness and ventilation duct shapes (Fan & Ahmadi, 1993; McFarland et al., 1997; You, R., Zhao, B., & Chen, C., 2012). Empirical equations require minimal information and computing effort, and the results can be reasonably good for engineering applications.

This paper reports our effort in predicting particle deposition in ECSs and APUs by using several empirical equations from previous studies. These equations allow us to account for the complex components of the ECS and APU. Furthermore, this investigation has compared the predicted results with corresponding experimental data for the deposition of particles of different sizes.

2 Method

The review in the previous section suggests that empirical equations are the best method for predicting particle deposition and penetration in the ECS and APU of an airliner. Although these systems differ from airplane to airplane, they have common components, and therefore generic models can be constructed. This section describes our effort in constructing general models for ECSs and APUs.

2.1 Particle deposition models

This investigation defined the total penetration of particles into an aircraft cabin:

$$P = \frac{C_{diffuser}}{C_{inlet}} \tag{1}$$

where $C_{diffuser}$ is the mass or number concentration of particles at the air diffusers in the aircraft cabin and C_{inlet} is the concentration at the inlet of the ECS or APU of the airplane. Accordingly, the total deposition of particle in the ECS and APU is

$\eta_d = 1 - P$.

In order to determine the particle deposition rate η_d in the ECS and APU of an airliner, this investigation combined several empirical equations obtained from previous studies after a comprehensive literature review. A detailed description of the empirical equations can be found in those studies (Fan & Ahmadi, 1993; McFarland et al., 1997; You, R., Zhao, B., & Chen, C., 2012). Here we show only the final forms of the equations.

You et al. (2012) developed several empirical equations for particle deposition on different types of smooth planar surfaces with various particle sizes (between 0.01 and 10 μm in diameter). For surfaces with complex shape, the model separates the surface into simple pieces to get the total deposition. These equations can be divided into four parts: the "fine" zone, the "coarse" zone, the "zero" zone, and the "transition" zone. The equations use a friction velocity u^*, which is defined as

$$u^* = u_m \sqrt{\frac{f}{2}} \tag{2}$$

where f is the friction factor that can be determined from the ASHRAE Handbook (Handbook, 2001):

If $f' \geq 0.018$, $f = f'$; otherwise, $f = 0.85 f' + 0.0028$.

$$f' = 0.11\left(\frac{k}{D} + \frac{68}{\mathrm{Re}}\right)^{0.25} \tag{3}$$

The "fine" zone is for particles with small diameters ($d_p < 0.0512(u^*)^{0.4227}$ μm). The size range varies with u^*, but in our calculation it was always smaller than 1 μm. The corresponding empirical equation for calculating the particle deposition velocity is

$$v_d = (5.15\times10^{-8}u^* - 5.63\times10^{-11})d_p^{-1.263} \tag{4}$$

The "coarse" zone is for particle sizes satisfying $d_p > 0.3577(\cos\theta)^{-0.41}$ μm or for particles that approach a surface with an attack angle θ smaller than 90° or cos θ greater than zero. The definition of attack angle θ is described in the investigation of You et al. (2012). The empirical equation for the particle deposition velocity is:

$$v_d = 3.7\times10^{-5} d_p^{1.9143}(\cos\theta) \tag{5}$$

The "zero" zone is for particles with $d_p > g(u^*, \cos\theta)$ μm or with an attack angle greater than *90*° or cos $\theta \leq 0$. The particle deposition velocity is zero:

$$v_d = 0$$

The function g for determining the d_p in the "zero" zone is defined as:

$$\log[g(u^*,\cos\theta)] = -0.941 + 0.796\log u^* + 0.333\cos\theta + 0.184(\log u^*)\cos\theta - 0.011(\log u^*)^2 + 0.15(\cos\theta)^2 \quad (6)$$

In cases none of the above conditions are satisfied, particles are in the "transition" zone. The empirical equation for calculating particle deposition velocity is:

$$v_d = f(u^*, \cos\theta, d_p)$$

where

$$\log[f(u^*,\cos\theta,d_p)] = -6.026 + 0.116\log u^* + 1.837\cos\theta + 1.079\log d_p - 0.653\log u^*\cos\theta - 0.89\log u^* \times \log d_p + 1.484\log d_p\cos\theta + 0.17(\log u^*)^2 - 0.074\cos^2\theta + 1.076(\log d_p)^2 \quad (7)$$

The calculated particle deposition velocity v_d on to the inner surfaces of a duct is then substituted into the following equation to obtain the particle deposition rate η through the duct.

$$\eta = v_d \frac{A}{V} \quad (8)$$

Determining the attack angle θ in a curved pipe by means of the above model is a complex process, and there are a large number of curved pipes in the ECS of an aircraft. Therefore, for curved pipes this investigation replaced the equations from You et al. (2012) with a semi-empirical equation from McFarland et al. (1997). The latter equation calculates particle penetration through a curved pipe by

$$P = \exp\left(\frac{4.61 + a\theta' St}{1 + b\theta' St + c\theta' St^2 + d\theta'^2 St}\right) \quad (9)$$

where

$$a = -0.9526 - 0.05686\,\delta, \quad b = \frac{-0.297 - 0.0174\delta}{1 - 0.07\delta + 0.0171\delta^2},$$
$$c = -0.306 + \frac{1.895}{\delta^{0.5}} - \frac{2}{\delta}, \quad d = \frac{0.131 + 0.0132\,\delta + 0.000383\,\delta^2}{1 - 0.129\,\delta + 0.0136\,\delta^2},$$
$$\delta = \frac{2R}{D}, \quad St = \frac{C_c \rho_p d_p^2 u_m}{9\mu D}, \quad C_c = 1 + \frac{\lambda}{d_p}[2.514 + 0.8\exp(-0.55\frac{d_p}{\lambda})].$$

The equations from You et al. (2012) were for pipes with smooth internal surfaces, while the equations developed by McFarland et al. (1997) neglect surface roughness.

In order to account for the roughness of the inner surfaces of the ECS in an old airplane, where particle had deposited significantly and the roughness could not be neglected, we replaced the equations of You et al. (2012) with empirical equations from Fan and Ahmadi (1993). That is,

$$v_d^+ = \min\{\ 0.14,\ \ 0.084\,Sc^{-2/3} + \frac{1}{2}[\frac{(0.64k^+ + \frac{1}{2}d^+)^2 + \frac{\tau_p^{+2} g^+ L_1^+}{0.01085(1+\tau_p^{+2}L_1^+))}}{3.42 + (\tau_p^{+2} g^+ L_1^+)/(0.01085(1+\tau_p^{+2}L_1^+))}]^{1/(1+\tau_p^{+2}L_1^+)}$$
$$\times[1+8e^{-(\tau_p^+-10)^2/32}]\frac{0.037}{1-\tau_p^{+2}L_1^+(1+(g^+/0.037))}\} \qquad (10)$$

In Eq. (10), $L_1^+ = 3.08/(Sd^+)$ and k^+ is the surface roughness, which can be calculated as $k^+ = \frac{ku^*}{\nu}$. The dimensionless particle relaxation time is $\tau_p^{+2} = \frac{C_c \rho_p d_p^2 u^{*2}}{18\rho\nu^2}$, and the dimensionless acceleration due to gravity is defined as $g^+ = \nu u^{*-3} g$. For a horizontal pipe, $g^+ = 0$ in Eq. (10), and the gravitational settling velocity g^+ should be added. With the dimensionless deposition velocity v_d^+ from Eq. (10), we obtain the particle penetration rate P for a pipe inner surface with significant roughness (relative roughness larger than 0.006) from

$$P = \exp(-\frac{4v_d^+ u^*}{d_o u_m} L) \qquad (11)$$

2.2 Geometric model of the ECS and APU

A geometric model of the ECS and APU in a commercial airplane, as shown in Figure 1, was created by use of the three-dimensional modelling software Gambit (ANSYS, 2006). This model consists of the key components of an ECS (an air-conditioning pack, a mix manifold, a main air distributor or manifold, and air diffusers) and an APU inlet. Many auxiliary components, such as anti-ice pipe lines and balance tubes, were neglected for the sake of simplicity. The model also shows the pipe that connects the ECS to the GAC.

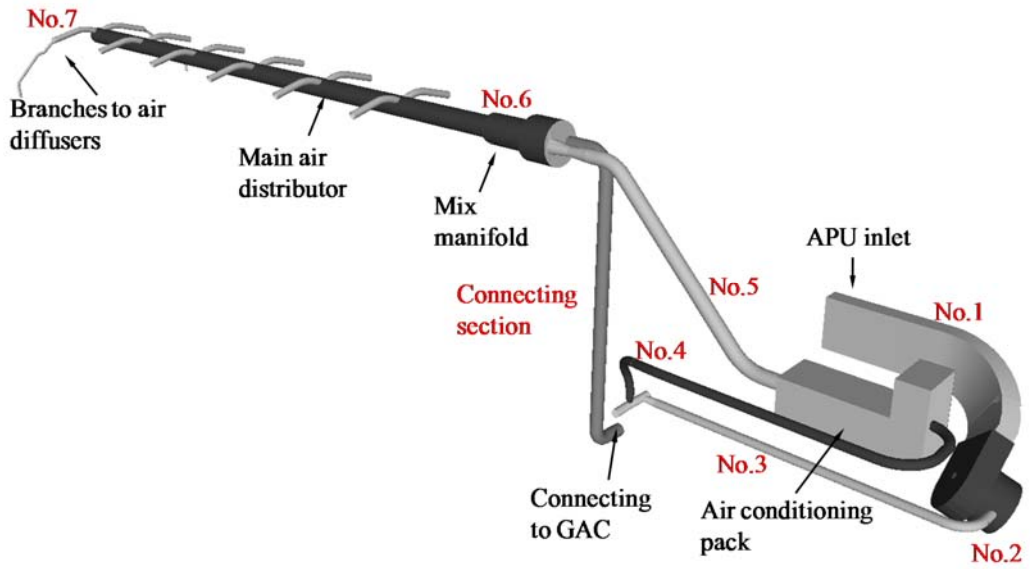

Fig.1. Geometric model of the ECS and APU

This investigation studied five types of commercial airplanes: a regional jet, a Boeing 737-800, an Airbus 319, an Airbus 320, and an MD-82. We divided the five types of airplanes into two groups based on the source fresh air: through APU or GAC. With APU, the simplified model for different airplanes was the same as most of the ECS were similar. With GAC, the air-conditioning pack and the connecting pipes were replaced with a straight pipe connecting the GAC and the airplanes. We evaluated the first four airplane types with the use of APUs to supply air to the cabin as shown in Table 1 (Wu & Zhao, 2007). The generic model in Figure 1 and the airflow rate were scaled according to the external dimensions of the various APUs.

Table 1. APU information for the different airplanes studied

Airliner	APU model	APU size (L×W×H mm)	Airliner size (L×W×H m)	Total supply air (kg/s)
Regional jet	----	812×534×655	33.46×27.29×8.44	0.84
Boeing 737-800	Model 131-9B	----	39.50×34.40×12.50	1.484
Airbus 319	APS3200, Model 131-9A	1247×853×757	37.57×34.09×11.76	1.475
Airbus 320	APS3200, Model 131-9A	1247×853×757	33.84×34.10×11.76	1.195

We divided the components of the air-conditioning pack in the ECS, such as fans and turbines, into various types of surfaces. The empirical equations shown in the previous section were then used to calculate the particle deposition on the components. Haghighi-Khoshkhoo and McCluskey (2007) found that particle deposition on heat exchangers was dependent only on geometry, and models already existed for particle deposition on the fin edge of the heat exchanger (Siegel & Nazaroff, 2003). We estimated the internal parameters of heat exchangers using the information from Chen et al. (2008) and predicted particle deposition by combining this information with a model from Siegel and Nazaroff (2003). The model is

$$\eta_d = (Stk_{fin}\frac{\pi}{2})\frac{t_{fin}}{w}cf \tag{12}$$

Our calculation of particle deposition inside the ECS and APU considered only the

physical process of deposition on various surfaces and neglected any chemical reactions that may occur there. This simplification may have led to a deviation between the calculated and measured particle deposition because of the volatilization and condensation of volatile or semi-volatile particle matter. The phase transition of volatile or semi-volatile particle matter may occur when the air flowed through ECS components such as the compressors or heat exchangers, where the temperature of the air and particles changes largely.

Our calculations of particle deposition divided the ECS and APU into seven sections as shown in Figure 1. Table 2 lists the geometric characteristics and corresponding empirical equations used for the regional jet, Boeing 737-800, Airbus 319, and Airbus 320. Since these airplanes were relatively new and the ECS was made of steel or aluminum (Chen, M.Y., Zhang, X.Y., & Cai, W. 2008; Yang, M., Ke, P., & Zhang, S., 2014), the absolute roughness was estimated to be 0.03 mm (Lu, 2008). Thus, Eqs. (4) – (9) and (12) were used to calculate the particle deposition as shown in Table 2.

Table 2. Geometrical characteristics and applied equations for each part of the ECS and APU

Type	Section No.	Section characteristic	Equations
Regional jet, Boeing 737-800, Airbus 319, Airbus 320	1	Oblique square and curved ducts	(4)–(9)
	2	Combination of complex geometric components	(4)–(8)
	3	Horizontal and curved pipes	(4)–(9)
	4	Horizontal and curved pipes	(4)–(9)
	5	Complex air-conditioning package with straight and curved pipes	(4)–(9), (12)
	6	Horizontal pipes with various diameters	(4)–(8)
	7	Straight and curved pipes and air diffusers	(4)–(9)
MD-82	Connecting section	Vertical and curved pipes	(4)–(9)
	6	Horizontal pipes with various diameters	(4)–(8)
	7	Straight and curved pipes and air diffusers	(9)–(11)

The MD-82 aircraft was a retired commercial airplane. This investigation assumed that a large number of particles had been deposited on the airplane's ECS, so that the surface roughness was very high. In addition, a GAC was used to supply air to the MD-82 airplane cabin, so that the GAC replaced both the APU and the air-conditioning pack in the ECS. The GAC was connected to the ECS of the airplane by means of a pipe, as shown in Figure 1. The airflow rate in the system was 4800 m^3/h. Particle deposition inside the GAC was not studied with the equations in this paper, but it was measured from experiment. Eqs. (9) – (11) for rough surfaces were used in the branch pipes of the ECS where the small pipe diameter caused a considerable increase in relative roughness, as shown in Table 2.

Particle deposition is related to the air velocity u_m or friction velocity u^* in the pipes. This study used equivalent pipe diameters and airflow rates to estimate the air velocity in each section of the ECS and APU. The Geometric model in Fig.2 indicates that each part of the ECS has very complex structure including pipes with different diameters. Table 3 only presents the representative radius and corresponding air velocity as calculated for different sections. Table 3 also shows the total inner surface area in the simplified model of each airliner.

Table 3. Radius and corresponding air velocity in different sections of the ECS and APU

Section No.	Prototype airliner		Boeing 737-800		Airbus 319		Airbus 320		MD-82	
	r (m)	u_m (m/s)	r (m)	u_m (m/s)	r (m)	u_m (m/s)	r (m)	u_m (m/s)	r (m)	u_m (m/s)
1	0.16	24.54	0.46	29.32	0.46	28.78	0.46	29.31		
2	0.14	67.74	0.38	82.98	0.38	81.43	0.38	82.94		
3	0.04	93.43	0.06	63.54	0.06	51.16	0.06	63.61	0.1*	37.97*
4	0.04	93.43	0.06	63.54	0.06	51.16	0.06	63.61		
5	0.07	13.03	0.11	10.54	0.11	7.14	0.11	8.82		
6	0.11	10.46	0.17	11.64	0.17	10.55	0.17	10.83	0.14	10.51
7	0.04	6.33	0.04	6.96	0.04	6.76	0.04	6.96	0.04	6.33
Inner surface area (m^2)	22.61		59.62		49.97		58.92		57.22	

* Connecting section between the GAC outlet and Section 6 in Figure 1.

Another parameter that significantly affects deposition is particle diameter. Since this paper used measured data (Cao et al., 2016) to validate the numerical results, the diameters were divided into the same categories as in the experimental data. In order to avoid repetition and make the validation more intuitively, this paper may change the way to show the measuerd data, such as transforming the figure into a table. Furthermore, as the experiments lasted for more than one year and there were several sets of measured data, this paper only listed part of the results for validation, but the experimental method was similar. For particle deposition in terms of mass concentration, this study used an aerodynamics diameter of 2.5 μm and 10 μm as representative of the $PM_{2.5}$ and PM_{10}, respectively. For particle deposition in terms of particle number, this study used the calculated number mean aerodynamics diameter 0.4 μm, 0.75 μm, 1.5 μm, 7.5 μm, and 10 μm to represent the measured mean particle number in size range of 0.3-0.5 μm, 0.5-1.0 μm, 1.0-2.0 μm, 2.0-5.0 μm, 5.0-10.0 μm, and > 10.0 μm, respectively.

3 Results

This section presents the results for particle deposition in the two types of systems classified in the previous section: (1) an ECS with an APU for the regional jet, Boeing 737-800, Airbus 319, and Airbus 320, and (2) an ECS with a GAC for the MD-82.

3.1 Particle deposition in the regional jet

As the regional jet was the prototype for the particle deposition model that was developed, the results for this aircraft are presented here. Table 4 shows the particle deposition percent rates in different sections of the ECS and APU for various particle sizes. The results indicate that the larger the particles were, the higher was the deposition percent rate. For example, over 95% of particles with a diameter greater than 10 μm were deposited in the sections before the mix manifold. The percent rate of deposition decreased as the particles became smaller. For fine particles with a diameter between 0.3 and 0.5 μm, the deposition rate before the mix manifold was as low as 2.3%. Table 4 also shows that the overall deposition percent rate of large particles in the ECS was nearly 100%, and that of fine particles was 75%.

Table 4. Calculated particle number deposition rates in the regional jet

Section No.	Description	0.3-0.5 μm	0.5-1.0 μm	1.0-2.0 μm	2.0-5.0 μm	5.0-10.0 μm	> 10 μm
1	Inlet to APU	0.0%	0.0%	0.1%	0.4%	1.8%	3.1%
2	Inside APU	0.8%	0.0%	0.2%	0.8%	3.4%	5.8%
3	Connecting pipes between APU and Section 4	0.7%	0.00%	0.5%	7.2%	37.6%	61.8%
4	Connecting pipes between Section 3 and air-conditioning pack	0.4%	0.1%	0.3%	6.1%	22.1%	19.5%
5	Air-conditioning pack to mix manifold	0.4%	0.2%	0.8%	5.7%	11.0%	4.9%
Deposition from outside to mix manifold		**2.3%**	**0.3%**	**1.9%**	**20.2%**	**75.9%**	**95.1%**
6	Mix manifold to branch pipe	49.1%	49.9%	49.2%	40.8%	13.1%	2.8%
7	Branch pipe to the tenth row	24.2%	24.7%	24.5%	21.6%	7.9%	1.7%
Total deposition percentage		**75.6%**	**74.9%**	**75.6%**	**82.6%**	**96.9%**	**99.6%**

Figure 2 shows the averaged ground particle size distribution outside the cabin of the regional during the flight. The $PM_{2.5}$ and PM_{10} mass concentration on that day from the air quality station closest to the airport were 133 μg/m^3 and 276 μg/m^3, respectively.

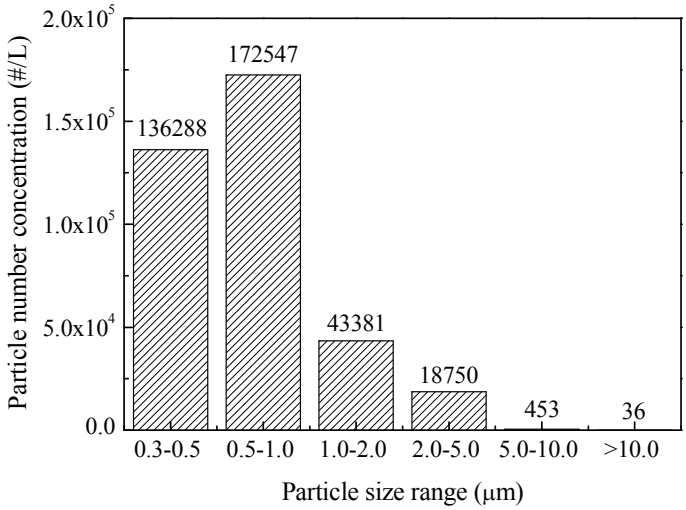

Fig. 2. Averaged particle size distribution outside the cabin of the regional jet during the flight

Table 5 compares the calculated particle deposition rate with the corresponding experimental data measured by Cao et al. (2016). Because the researchers only conducted the measurement in the regional jet for once, this paper does not have an error bar. The measured particle deposition was the difference between particle concentrations measured inside and outside the cabin. The measurements were conducted while the regional jet was on the ground with the APU operating to supply outside air to the cabin.

Table 5. Comparison of calculated particle deposition and experimental data for the regional jet

Particle size range	Measured deposition %	Calculated deposition %	Difference %
0.3-0.5 μm	82.3	75.6	**8.3**
0.5-1.0 μm	98.7	74.9	**24.1**
1.0-2.0 μm	99.2	75.6	**23.7**
2.0-5.0 μm	97.5	82.6	**15.4**
5.0-10.0 μm	78.4	96.9	**23.7**
> 10.0 μm	100.0	99.6	**0.4**

The differences between the calculated and measured results for the regional jet may have arisen from the simplifications used in the geometric model or the empirical equations for particle deposition. In addition, the experimental measurements were not free of errors, as the measured particle deposition rate did not show a positive correlation with particle size. A positive correlation has been confirmed in many other experimental studies (Sippola & Nazaroff, 2002). In light of the uncertainties in this investigation, the agreement between the calculated results and the measured data was reasonably good, but the models should be further improved in the future.

In addition, this particular airplane may not be typical of commercial aircraft at major Chinese airports. In order to make our investigation more relevant and universal, we studied particle deposition in the ECSs of different kinds of airplanes.

3.2 Particle deposition in the MD-82 airplane

This section compares the calculated particle deposition in the ECS of the MD-82 airplane with the corresponding measured data (Cao et al., 2015). Because air was supplied to the MD-82 by a GAC, the geometric model of the ECS did not have an APU and an air-conditioning pack. Instead, it had a connecting section between the GAC outlet and the mix manifold as shown in Figure 1.

Table 6 shows the calculated particle deposition percent rate for each section. The trend in particle deposition in the ECS of the MD-82 was similar to that in the regional jet (Table 4). The results indicate that the deposition of large particles occurred mainly in the upstream sections of the ECS. Table 7 compares the experimental data for particle deposition in the MD-82 airplane with the calculated deposition rates, in which particle deposition in the GAC has been taken into account. Once again, the results obtained with our empirical particle deposition model differed from the experimental data by less than 20%, except when the particle size was very small.

Table 6. Calculated particle number deposition in the ECS of the MD-82 airplane

Section No.	Description	0.3-0.5 μm	0.5-1.0 μm	1.0-2.0 μm	2.0-5.0 μm	5.0-10.0 μm	> 10 μm
1	Inlet to mix manifold	0.8%	0.4%	1.2%	12.2%	50.5%	73.6%
6	Mix manifold to branch pipe	0.4%	0.2%	0.8%	3.4%	7.7%	6.7%
7	Branch pipe to the tenth row	12.8%	13.0%	14.1%	21.5%	24.8%	15.4%
Total deposition percentage %		**14.0%**	**13.6%**	**16.1%**	**37.1%**	**83.0%**	**95.7%**

Table 7. Comparison of calculated and measured particle deposition in the ECS and GAC for the MD-82 airplane

Particle size range	Measured deposition %	Calculated deposition %	Difference %
0.5-1.0μm	20.6	13.6	**33.9**
1.0-2.0μm	17.2	16.1	**6.6**
2.0-5.0μm	31.7	37.1	**16.4**
5.0-10.0μm	91.3	83.0	**9.1**
> 10.0μm	92.9	95.7	**3.1**

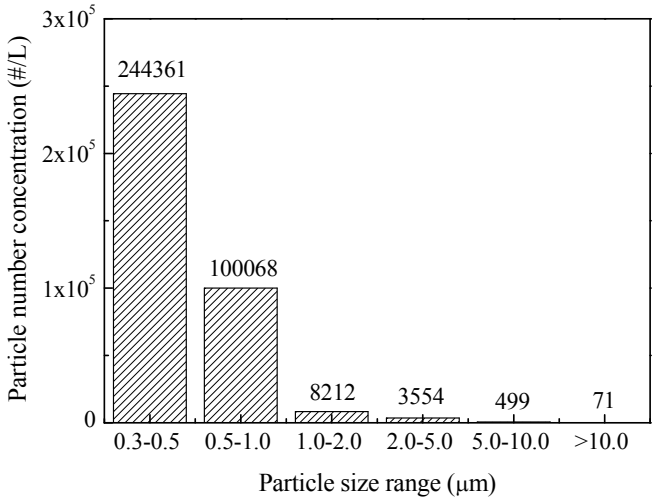

Fig.3. Particle size distribution outside the MD-82

The particle deposition percent rates shown in Table 7 were measured on a day when the $PM_{2.5}$ mass concentration outside the MD-82 airplane was 178 μg/m^3, and in figure 3 is the particle size distribution. There were many uncertainties in the measured data. For example, the particle deposition in the GAC was measured on another day, when the $PM_{2.5}$ mass concentration outside the cabin was 176 μg/m^3. Although the $PM_{2.5}$ mass concentrations were similar on the two days, the particle sizes, numbers, and even chemical components may be different. The PM_{10} deposition in the GAC was estimated by the same way. Furthermore, the empirical models used in this study incorporated many approximations, and the geometric model was not highly accurate. In light of these uncertainties, a discrepancy of 20% or less is quite good. However, we were unable to identify the cause of the large difference between the calculated and measured deposition for fine particles. This difference should be investigated in the future.

3.3 Particle deposition in the ECSs of commercial flights

The results of the calculations in the previous two sections were consistent with the measured deposition percent rates, but the regional jet and MD-82 airplane were not in commercial operation. To determine the applicability of our model to commercial flights, we compared the calculated particle deposition in the Boeing 737-800, Airbus 319, and Airbus 320 airplanes, which serve major airports in China where there is heavy pollution. Particle deposition in different parts of these airplanes was assumed to follow a similar pattern to that in the regional jet, but with a different magnitude.

Table 8 compares the calculated particle deposition percent rates with the corresponding experimental data for $PM_{2.5}$ and PM_{10} mass concentrations measured during flights by Cao et al. (2016). The differences between the calculated and measured particle deposition percent rates was also acceptable, by less than 15%.

Table 8. Comparison of calculated and measured particle deposition in commercial airplanes

Date	Route	Location	Airplane	Particle size	Measured deposition %	Calculated deposition %	Difference %
Sep. 22, 2014	Tianjin to Xi'an	Tianjin	Airbus 319	2.5 μm	76.6	76.9	**0.5**
				10 μm	88.1	97.0	**10.0**
Sep. 24, 2014	Xi'an to Tianjin	Xi'an	Boeing 737-800	2.5 μm	71.4	76.8	**7.5**
				10 μm	85.3	97.6	**14.4**
Nov. 10, 2014	Tianjin to Chongqing	Tianjin	Airbus 320	2.5 μm	88.7	77.1	**13.0**
				10 μm	89.3	97.6	**9.3**

For all the three flights, there was very good agreement between calculated and measured particle deposition. However, it was very strange that, for Airbus 319 and 320 (two somehow similar airlines), the difference of the measured deposition for 2.5 μm particles was 12% while for 10 μm particles there was almost no difference. The difference in different time of measurements, human activities and measurement errors can be the reasons for the difference in measuring $PM_{2.5}$ particles. For PM_{10}, the deposition rate was always close to 100% so the difference was small anyway.

However, the differences still deserve our attention. For the particle mass concentration outside the cabin, we used the data from the air quality monitoring station closest to a given airport (CNEMC, 2014). The distance between the air quality monitoring station and the airport was 3 km for Tianjin, 10 km for Xi'an. The particle mass concentration may not have been the same at the air quality monitoring station and the airport because of the distance between them. Figure 4 compares the $PM_{2.5}$ concentration measured at Tianjin Airport with that measured at the air quality monitoring station closest to the airport. The air quality monitoring station measures $PM_{2.5}$ with it heated system to avoid the effects of water condensation on the particles, but our measurements measure wet samples which will be sensitive to humidity. The difference in instruments will in some extent lead to deviations. A very significant difference was found at some of the measurement times, even though the distance to the monitoring station was smaller between the two airports.

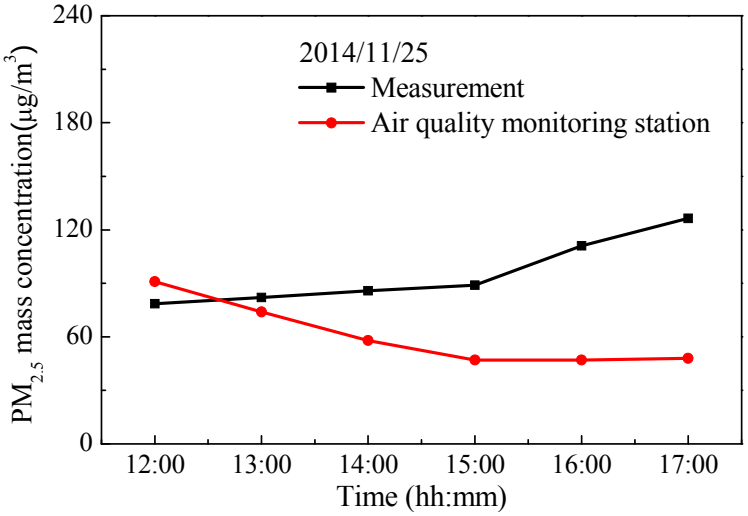

Fig.4. $PM_{2.5}$ mass concentration from our measurement at Tianjin Airport and from the air quality monitoring station closest to the airport.

In addition, because of flight regulations that restrict where passengers' belongings can be placed in a cabin, our instrument could be placed only on the seat table. All the measurements were performed by the same person. We suspect that the breath from the person may have had an impact on the accuracy of the measured data. This was because the human breath may bring in some expiratory droplets and added to the final measured particle mass concentration. In order to verify this assumption, the particle mass concentration monitor was placed on a table far from a person for 20 minutes, and then the person sat close to the table for 50 minutes as he would do during a flight. The measured data in Figure 5 indicates that the breath of the person could increase the particle mass concentration by 20%. Other researchers have also found that human breathing and other activities can produce particles of different sizes (Papineni & Rosenthal, 1997; McDonagh & Byrne, 2014).

In light of the uncertainties described above, the comparison between the calculated and measured particle deposition percent rates for real flights is good.

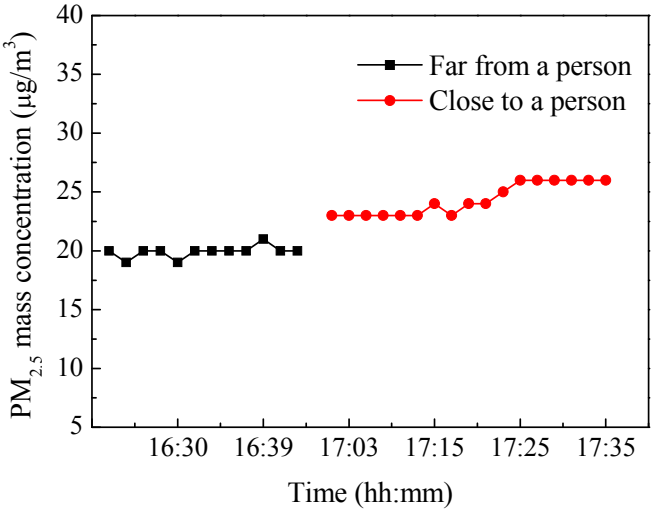

Fig.5. Effect of human breath on $PM_{2.5}$ mass concentration

4 Discussion

Although the particle deposition calculated for different types of airplanes, as shown in Section 3, was reasonably accurate when compared with the measured data as we decided that the comparison with a difference smaller than 35 % was acceptable, the model may need further development. For example, many details were neglected in the geometrical model shown in Figure 1. It is in these details that particles are likely to be trapped.

Another major assumption was the roughness of the inner surfaces of the ECS. Because the commercial airplanes in operation in this investigation were relatively new, we used the surface roughness of new materials. In actual fact, since the outside air at most Chinese airports is heavily polluted, there may have been large numbers of particles deposited on the ECS surfaces. It was very difficult to obtain the correct roughness for our calculations. In the case of the old MD-82 airplane, the absolute roughness was determined to be 0.15 mm (Lu, 2008). This value may also have been too low, considering the age of the airplane. These uncertainties were unfortunate because surface roughness was an important parameter in determining the particle deposition rate in our study. The surface roughness of the ECS should be further studied.

Furthermore, this investigation assembled the empirical equations for particle deposition from various studies. These equations do not always produce the same results under the same conditions. Table 9 compares the $PM_{2.5}$ mass penetration rate in a horizontal round pipe as calculated by the empirical equations from You et al. (2012) and Fan and Ahmadi (1993). The interior surface of the pipe was assumed to be smooth. There was a difference of 6.2% between the results of the two equations. It is difficult to determine which empirical equation is actually better, since both sets of authors published very good results. In addition, our case is more complicated than their examples, making an "apple to apple" comparison impossible. Further validation of the empirical equations is essential for each component of an ECS. On the other hand, all the empirical models were developed for indoor environment with a much smaller air velocity than that in the ECS of an airplane. The high air velocity may have influence on the deposition and resuspension of the particles and lead to the differences between the calculated particle deposition rate and the actual one found in our measurements.

Table 9. Particle penetration in a simple pipe with two empirical equations

Empirical equation	Particle size	Pipe diameter	Pipe length	Penetration percent rate	Difference
You et al. (2012) Fan and Ahmadi (1993)	2.5 μm	0.2 m	2 m	98.0 % 92.3 %	6.2 %

Particle resuspension from the inner surface of the duct of also had non-negligible effects on particle deposition in the ECS of an aircraft. Zhou et al. (2011) did the investigation on particle resuspension in ventilation duct and indoor surfaces. Their study shows that when air flows through the ducts, there is possibility that particles deposited on the inner surfaces are carried away and larger particles have a larger possibility to get resuspended. In our study, the resuspended particles finally get into the aircraft cabin which may lead to a decrease of the measured particle deposition percent rate and affect the accuracy of the model. Further investigation of particle resuspension is necessary to be considered in the model.

In order to show the severity of particle deposition inside the ECS of the aircraft more obviously, Figure 6 compares the particle mass concentration inside and outside the cabins for three commercial airplanes. The results show that the large amount of particle deposition inside the ECS of aircrafts may be harmful for the operation of the system and reduce the service life of the corresponding parts.

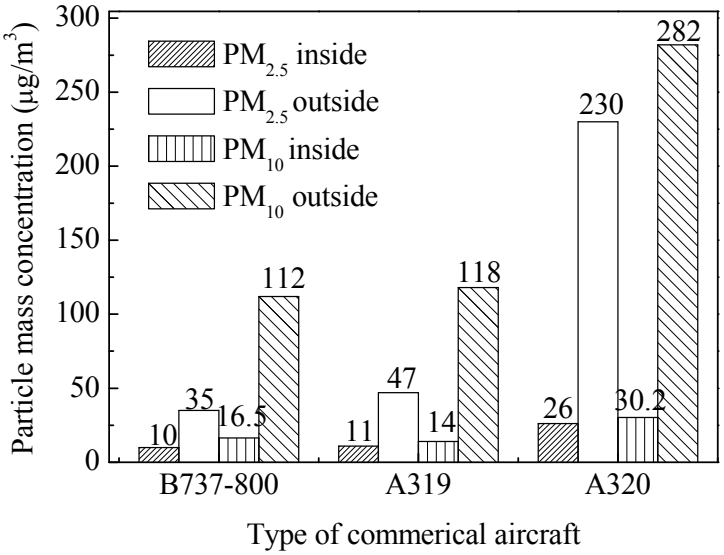

Fig.6. Relationship between particle mass concentration inside and outside the three types of commercial aircraft

5 Conclusion

This investigation developed a generic particle deposition model for the ECS in five types of aircraft: a regional jet, an MD-82, a Boeing 737-800, an Airbus 319, and an Airbus 320. This study used the model to calculate deposition percent rates in the ECS for a range of particle sizes. The largest difference between the calculated deposition percent rate and the corresponding experimental data was generally less than 35%. Thus, the simplified deposition model is able to provide reasonably good predictions.

This study also used the model to predict the particle mass deposition rate in commercial airplanes. The differences between the calculated and measured $PM_{2.5}$ and PM_{10} particle deposition were less than 15%. In light of the uncertainties in the model and the measurements, the difference should be acceptable.

Our calculated particle deposition rates show that almost all the large particles (5 μm or larger in diameter) were deposited in the ECS. The deposition rate decreased with a decrease in particle diameter, but the deposition rate for particle number remained as high as 75% for fine particles (0.3 μm in diameter). Most of the particle deposition occurred near the entrance of the ECS, where the geometry was the most complex.

Acknowledgements

The research presented in this paper was financially supported by the National Basic Research Program of China (the 973 Program) through Grant No. 2012CB720100.

References

ANSYS (2006). ANSYS Gambit version 2.4.6. ANSYS, Inc., Lebanon, NH.

Cao Q, Liu Y, Liu W, Lin C.H, Baughcum S, Norris S, Wei D, Long Z, Shen X, Chen Q (2016). Experimental study of particle deposition in the environmental control systems of commercial airliners. *Building and Environment*,96:62-71.

Chen M, Zhang X, Cai, W (2008). Operating analysis of airplane air conditioning heat exchanger. *Journal of Shanghai University of Engineering Science*.

CNEMC (2014). Air quality report of 74 cities in the first half year of 2013.

http://www.cnemc.cn/publish/totalWebSite/news/news_37029.html.
Fan F G, Ahmadi G (1993). A sublayer model for turbulent deposition of particles in vertical ducts with smooth and rough surfaces. *Journal of Aerosol Science,* 24: 45-64.
Flightstats (2014). Airline performance reports. http://www.flightstats.com/.
Haghighi-Khoshkhoo R, McCluskey F (2007). Air-side fouling of compact heat exchangers for discrete particle size ranges. *Heat Transfer Engineering,* 28:58-64.
Handbook A (2001). Fundamentals. *American Society of Heating, Refrigerating and Air Conditioning Engineers, Atlanta,* 111.
Kan H, Chen B, Hong C (2009). Health impact of outdoor air pollution in China: current knowledge and future research needs. *Environmental Health Perspectives,* 117: A187.
Lai A C K (2003). Particle deposition indoors: a review. *Indoor Air,* 12: 211-214(214).
Lu Y (2008). Practical Heating, Air-Conditioning System Design Manual. China Architecture & Building Press. (in Chinese)
McDonagh A, Byrne M A (2014). A study of the size distribution of aerosol particles resuspended from clothing surfaces. *Journal of Aerosol Science,* 75: 94-103.
McFarland A R, Gong Muyshondt, Wente WB, Anand, NK. (1997). Aerosol deposition in bends with turbulent flow†. *Environmentalence & Technology,* 31: 3371-3377.
Papineni R S, Rosenthal F S (1997). The size distribution of droplets in the exhaled breath of healthy human subjects. *Journal of Aerosol Medicine,* 10: 105-116.
Shanghai CS Capital (2013). http://www.cscapital.cn/.
Siegel J A, Nazaroff W W (2003). Predicting particle deposition on HVAC heat exchangers. *Atmospheric Environment,* 37: 5587-5596.
Sippola M R, Nazaroff W W (2002). Particle deposition from turbulent flow: Review of published research and its applicability to ventilation ducts in commercial buildings. *Lawrence Berkeley National Laboratory*.
Sun K, Lu L, Jiang H (2011). A computational investigation of particle distribution and deposition in a 90° bend incorporating a particle–wall model. *Building and Environment,* 46: 1251-1262.
Tian L, Ahmadi G (2007). Particle deposition in turbulent duct flows—comparisons of different model predictions. *Journal of Aerosol Science,* 38: 377-397.
Wang M, Lin C H, Chen Q (2011). Determination of particle deposition in enclosed spaces by Detached Eddy Simulation with the Lagrangian method. *Atmospheric Environment,* 45: 5376–5384.
Wu J, Zhao B (2007). Effect of ventilation duct as a particle filter. *Building and Environment,* 42: 2523-2529.
Yang M, Ke P, Zhang S (2014). Preliminary investigation of the effect of aircraft ECS to the bleed air contamination: numerical tool development, 44th International Conference on Environmental Systems.
You R, Zhao B, Chen C (2012). Developing an empirical equation for modeling particle deposition velocity onto inclined surfaces in indoor environments. *Aerosol Science and Technology,* 46: 1090-1099.
Zhao B, Chen J (2006). Numerical analysis of particle deposition in ventilation duct. *Building and Environment,* 41: 710-718.
Zhang J, Li A, Li D (2008). Modeling deposition of particles in typical horizontal ventilation duct flows. *Energy Conversion and Management,* 49: 3672-3683.
Zhou B, Zhao B, Tan Z (2011). How particle resuspension from inner surfaces of ventilation ducts affects indoor air quality—a modeling analysis. *Aerosol Science and Technology,* 45: 996-1009.